Zhao, X., Liu, W., Lai, D., and Chen, Q. 2018. "Optimal design of an indoor environment by the CFD-based adjoint method with area-constrained topology and cluster analysis," *Building and Environment*, 138: 171-180.

Optimal Design of an Indoor Environment by the CFD-based Adjoint Method with Area-Constrained Topology and Cluster Analysis

Xingwang Zhao [a], Wei Liu [b,*], Dayi Lai [a], and Qingyan Chen [c, a]
[a]Tianjin Key Laboratory of Indoor Air Environmental Quality Control, School of Environmental Science and Engineering, Tianjin University, Tianjin 300072, China
[b]School of Civil Engineering, ZJU-UIUC Institute, Zhejiang University, Haining 314400, China
[c]School of Mechanical Engineering, Purdue University, West Lafayette, IN 47907, USA

*Corresponding author email address: weiliu@intl.zju.edu.cn

ABSTRACT
An indoor environment should be designed to provide occupants with a desirable level of thermal comfort and air quality. The optimal design of an indoor environment can be achieved by using the computational fluid dynamics (CFD)-based adjoint method to determine the size, locations, and shape of air supply inlets, and the air supply parameters (i.e., velocity, temperature, and angle). However, the optimal design may involve a large number of air supply inlets, which would be impractical to implement. This investigation developed an area-constrained topology and cluster analysis to consolidate multiple air supply inlets into a limited number and to determine their size and locations. The desired indoor environment can be maintained by further optimizing the air supply inlet shape and parameters. This investigation demonstrated the method's capability by applying it to a two-person office and a single-aisle, fully-occupied aircraft cabin. The optimal thermal comfort conditions around the occupants can be achieved with a limited number of air supply inlets at appropriate locations.

Keywords: Indoor environment; CFD-based adjoint method; Area-constrained topology; Cluster analysis; Location optimization.

1. Introduction
In a survey of human activity patterns, Klepeis et al. [1] found that people in the United States spent an average of 87% of their time inside buildings. It is therefore very important to create a comfortable, healthy, energy-efficient, and productive indoor environment. Such an indoor environment is usually created by heating, ventilating and air-conditioning (HVAC) systems. In the United States, heating of building spaces accounts for 37% of the total building energy consumption, and cooling of spaces accounts for 10%; in turn, the total energy use in buildings accounts for 41% of the country's primary energy consumption [2]. Even with such high energy usage, the indoor environments created were found to be unsatisfactory in nearly a quarter of U.S. residences [3]. Thus, it is crucial to design an HVAC system with optimal air supply conditions that provides a desirable indoor environment.

Conventional design of an indoor environment uses a trial-and-error process [4]. The process requires tens of trials to adjust the HVAC system parameters for creation of a better environment. Even with such a dedicated effort, the final design may not be optimal. Recently, many researchers have attempted to use optimization methods such as the genetic algorithm (GA) method [5], artificial neural network (ANN) method [6], proper orthogonal decomposition (POD) [7], and adjoint method [8]. For design of an indoor environment, all the above methods would require the use of computational

fluid dynamics (CFD) for determining the air distributions. This is because CFD is the most accurate and informative tool for predicting indoor air distributions [9]. Thus, most recent optimizations have been CFD-based, as summarized by Chen et al. [10].

Chen et al. [10] compared different CFD-based optimization methods and found that the CFD-based GA method could find the globally optimal solution with high accuracy, but its computing time was equivalent to 20 times that of the adjoint method, and its computing time was proportional to the number of design variables [11]. The CFD-based ANN method performs CFD simulations of multiple representative cases to train the ANN. With a well-trained ANN, the design objectives can be obtained without using any CFD simulations in the design procedure, and thus this method can be highly efficient. However, the prediction error of the ANN may reduce the accuracy of design results [12]. The CFD-based POD method establishes cause-effect maps between the design variables and the design objectives using a number of CFD simulations as samples. With this mapping relationship, the POD method can directly provide a design objective for a given design variable, thus speeding up the calculation. However, the accuracy of the POD method also depends on the number of samples used [13]. The CFD-based adjoint method is a gradient-based optimization method that computes the gradient of the objective function over the design variables to provide the search direction. Thus, the CFD-based adjoint method can quickly find the optimal value, and the computing time does not change with the number of design variables, although it may fall into local optima [4]. By means of the above comparison, this study identified the CFD-based adjoint method as a suitable approach for designing an indoor environment.

Liu et al. [14, 15] used the CFD-based adjoint method to identify the air supply inlet size and location and air supply parameters for a ventilated cavity and an aircraft cabin. They fixed the number of air supply inlets and assumed the inlet shape to be rectangular during the design process. For an optimal indoor environment, the number of air supply inlets may be unknown in advance, and the air supply inlet can take any shape. Therefore, the present investigation further developed the CFD-based adjoint method to determine the number, size, locations, and shape of the air supply inlets and the corresponding air supply parameters.

2. Methods

Using the CFD-based adjoint method to design an indoor environment, this study first needed to construct an objective function for the design objectives. There are multiple design objectives for an indoor environment, such as thermal comfort, air quality, and energy efficiency, etc. For the purpose of demonstration, this study used thermal comfort as the design objective. The thermal comfort level in an indoor environment can be quantitatively defined by the predicted mean vote (PMV) [16] and the predicted dissatisfied percentage (PD) due to draft [17]. The closer to zero the PMV and PD are, the better the thermal environment is. Therefore, this study normalized each criterion and constructed a single objective function by using weighting factors as shown in Eq. (1):

$$J(\xi) = w_1 \frac{\int_\Theta \frac{PMV^2}{9} d\Theta}{\int_\Theta d\Theta} + w_2 \frac{\int_\Theta \frac{PD}{100} d\Theta}{\int_\Theta d\Theta} \quad (1)$$

where J is the objective function; ξ a vector that denotes the design variables, such as air supply velocity, $\mathbf{V}_{inlet}$, air supply temperature, T_{inlet}, and number, size, locations, and shape of the air supply inlets; Θ the design domain of the indoor environment; and w_1 and w_2 the weighting factors. This investigation used values for w_1 and w_2 from Ncube and Riffat [18], who conducted a questionnaire survey in offices and found $w_1 = 0.455$ and $w_2 = 0.545$. The goal of the inverse design in this study was to identify the optimal ξ that ensured a minimal objective function J.

2.1. CFD-based adjoint method

To minimize the objective function, the CFD-based adjoint method started with initialized design variables and conducts CFD simulations to check whether or not the objective function was sufficiently small. If not, the method calculated the gradient of the objective function over the design variables. Since the design variables were not explicitly included in the objective function, it was impossible to find the relationship between the objective function and the design variables directly. To obtain the gradient, the adjoint method introduced an augmented objective function L as shown in Eq. (2).

$$L = J + \int_{\Omega} \left(P_a, \mathbf{V_a}, T_a \right) \mathbf{N} d\Omega \tag{2}$$

where Ω was the computational domain; P_a, $\mathbf{V}_a$, and T_a the adjoint pressure, adjoint velocity, and adjoint temperature, respectively; and $\mathbf{N}$ the incompressible Navier-Stokes equations in vector form.

The gradient of the augmented objective function over the design variables could be expressed as Eq. (3). Direct calculation of the gradient of the augmented objective function over the air velocity V, air temperature T, and pressure P was very difficult. Therefore, the adjoint method set the last three terms of Eq. (3) to zero, as expressed by Eq. (4). From Eq. (4), this study derived the adjoint equations as shown in Eqs. (5), (6), and (7). By numerically solving the Navier-Stokes equations and the adjoint equations alternatively, we could calculate the gradient of the objective function over the design variables using Eq. (8).

$$\frac{dL}{d\xi} = \frac{\partial L}{\partial \xi} + \frac{\partial L}{\partial P}\frac{\partial P}{\partial \xi} + \frac{\partial L}{\partial \mathbf{V}}\frac{\partial \mathbf{V}}{\partial \xi} + \frac{\partial L}{\partial T}\frac{\partial T}{\partial \xi} \tag{3}$$

$$\frac{\partial L}{\partial P}\frac{\partial P}{\partial \xi} + \frac{\partial L}{\partial \mathbf{V}}\frac{\partial \mathbf{V}}{\partial \xi} + \frac{\partial L}{\partial T}\frac{\partial T}{\partial \xi} = 0 \tag{4}$$

$$-\nabla \cdot \mathbf{V}_a = 0 \tag{5}$$

$$-\nabla \mathbf{V}_a \cdot \mathbf{V} - \left(\mathbf{V} \cdot \nabla \right) \mathbf{V}_a - \nabla \cdot \left(2\nu D\left(\mathbf{V}_a \right) \right) + \nabla P_a + T_a \nabla T + \mathbf{A} = 0 \tag{6}$$

$$-\left(\mathbf{V} \cdot \nabla \right) T_a + \nabla \cdot \left(\kappa \nabla T_a \right) - \gamma \left(\mathbf{V}_a \cdot \mathbf{g} \right) + B = 0 \tag{7}$$

$$\frac{dL}{d\xi} = \frac{\partial J}{\partial \xi} + \int_{\Omega} \left(P_a, \mathbf{V_a}, T_a \right) \frac{\partial \mathbf{N}}{\partial \xi} d\Omega \tag{8}$$

$$\xi_{k+1} = \xi_k - \lambda_k \frac{dL}{d\xi_k} \tag{9}$$

where ν is the effective viscosity; κ the effective thermal conductivity, **g** the gravity vector; γ the thermal expansion coefficient of air; **A** and B the source items in the adjoint momentum equations; λ the adaptive step size [19]; and k a positive integer. Next, we update the design variables for each initial air supply inlet cell using the steepest descent method [20] as shown in Eq. (9). This process was repeated until the objective function was sufficiently small.

The adjoint method could determine the movement of each cell individually within the air supply inlet. If the number of air supply inlets is fixed [14, 15], the movements of all the cells within the air supply inlet needed to be averaged. Then, the adjoint method changes only the size and location of the air supply inlet as shown in Fig. 1 (red dashed line). However, the optimal air supply inlet number may be variable, and the air supply inlets could take any shape. If we let each cell within the air supply inlet move individually, the design would lead to many small air supply inlets as shown in Fig. 1 (black regions), which is not realistic in an engineering application. Determination of the optimal and reasonable number, location, and shape of air supply inlets requires further investigation.

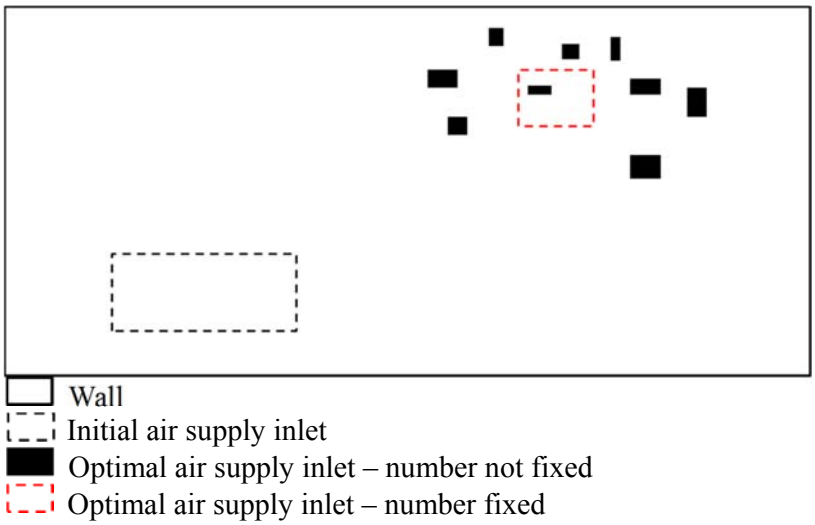

Fig. 1. Inverse design of air supply inlets by the CFD-based adjoint method

2.2. Determination of number, location, and shape of air supply inlets

To determine the optimal and reasonable number, location, and shape of air supply inlets, this study investigated an area-constrained topology optimization method [21]. The method was originally used to identify the optimal solid material distribution in a given space. The size of the region occupied by the solid material is determined by an additional area constraint for two-dimensional space or an additional volume constraint for three-dimensional space. For example, the integrated area-constrained topology optimization method and the CFD-based adjoint method were used to design optimal cantilever beam structure [22], duct structure [23] and the manifold structure of a 12-cylinder engine [24]. The results indicate that the constrained topology optimization method can effectively determine the structure, size and shape of industrial products and achieve the optimal designs. Therefore, this study integrated this method with the CFD-based adjoint method to determine the optimal number, size, locations, and shape for air supply inlets with constrained area.

The integrated method first conducts the inverse design process with the CFD-based adjoint method and updates the air supply velocity and temperature for each cell within the air supply inlet independently. The initial air supply inlet area covers all the potential locations. For example, this study specified one wall, *D*, as the initial air supply inlet as shown in Fig. 2. After a certain number of design cycles, each air supply inlet cell has different air supply parameters. The method then adds an area constraint to eliminate those cells with very low air velocity. This study used recommended ranges for air supply velocity [25] and air changes per hour to determine the area constraint. The area constraint can be expressed by

$$S_{min} \le S_{inlet} \le S_{max} \tag{10}$$

$$S_{min} = \frac{n_{min} \cdot Vol}{3600 \cdot V_{max}}; S_{max} = \frac{n_{max} \cdot Vol}{3600 \cdot V_{min}} \tag{11}$$

$$S_{inlet} = \int_D A_{cell_i} \cdot H\left(cell_i\right) dD \tag{12}$$

$$H\left(cell_i\right) = \begin{cases} 1 & if\ \ cell_i \in O \\ 0 & if\ \ cell_i \in D \setminus O \end{cases} \tag{13}$$

where S_{inlet} is the final air supply inlet area; S_{min} and S_{max} are the lower and upper bounds of the air supply inlet area constraint, respectively; n_{min} and n_{max} the lower and upper bounds of the recommended range of the air changes per hour, respectively; $\boldsymbol{V}_{min}$ and $\boldsymbol{V}_{max}$ the lower and upper bounds of the recommended range of the air supply velocity, respectively; Vol the room volume; $cell_i$ cell i of the initial air supply inlet; $H(cell_i)$ the Heaviside function that represents discrete value 0 or 1, taking the value of 1 for open cells and 0 for closed cells; and O the optimal air supply inlets.

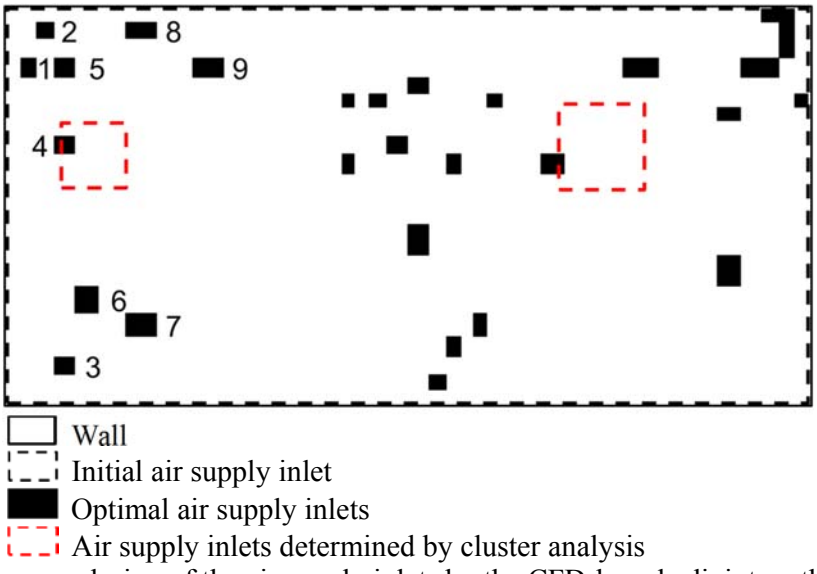

Fig. 2. Inverse design of the air supply inlets by the CFD-based adjoint method with area-constrained topology and cluster analysis

The black cells in Fig. 2 are the open cells, and the other cells are closed. Theoretically, the air supply inlet could take any shape. However, the example shows only rectangular openings because structured grid was used. The resulting optimal design in Fig. 2 is still impractical because of the scattered open cells and varying

parameters of the air supply from the inlets.

To solve the above-mentioned problem, this investigation used the centroid-based hierarchical cluster analysis for consolidating cells, because centroid-based algorithms can improve the quality and efficiency of clustering [26]. Cluster analysis treats each air supply inlet as a singleton cluster and calculates the distance between any two clusters using Eq. (14). The two clusters with the smallest distance are then selected and merged into one new cluster. During this clustering process, we determine the center of each new cluster with a flow-rate-weighted average as shown in Eq. (15), and air velocity and temperature by area-weighted average as shown in Eq. (16). Weighted averages are used because the location, area, velocity, and temperature for the air supply inlets are different.

$$d_{ij} = \sqrt{\left(x_i - x_j\right)^2 + \left(y_i - y_j\right)^2} \tag{14}$$

$$x_{ij} = \frac{A_i \cdot V_{z,i} \cdot x_i + A_j \cdot V_{z,j} \cdot x_j}{A_i \cdot V_{z,i} + A_j \cdot V_{z,j}}; y_{ij} = \frac{A_i \cdot V_{z,i} \cdot y_i + A_j \cdot V_{z,j} \cdot y_j}{A_i \cdot V_{z,i} + A_j \cdot V_{z,j}} \tag{15}$$

$$\mathbf{V}_{ij} = \frac{A_i \cdot \mathbf{V}_i + A_j \cdot \mathbf{V}_j}{A_i + A_j}; T_{ij} = \frac{A_i \cdot T_i + A_j \cdot T_j}{A_i + A_j} \tag{16}$$

where d_{ij} is the distance between clusters i and j; (x_i,y_i) and (x_j,y_j) are the center locations of clusters i and j, respectively; (x_{ij},y_{ij}) the center location of the new cluster, ij; A_i and A_j the areas of clusters i and j, respectively; $V_{z,i}$ the normal velocity of cluster i; $\mathbf{V}_i$ and $\mathbf{V}_j$ the velocities of clusters i and j, respectively; T_i and T_j the temperatures of clusters i and j, respectively; $\mathbf{V}_{ij}$ the velocity of new cluster ij; and T_{ij} the temperature of new cluster ij. When the above process is repeated, all the air supply inlets successively merge, eventually, into a required number of air supply inlets. If two air supply inlets are required, then the two inlets with a certain size ought to be located as shown by the two red dashed squares in Fig. 2. A square shape was used here for two inlets for the purpose of demonstration. Please note that before the cluster analysis, the velocity for different grid is different to give sufficient freedom for the design. The cluster analysis consolidates the air supply inlet cells and gives only uniform air supply parameters for each air supply inlet, although the method can give different parameters for each grid that may not be practical in design

After determining the air supply inlets by cluster analysis as described above, this study calculated the objective function. If the objective function was not sufficiently small, then this study fixed the number of air supply inlets and further designed the inlet shape and air supply parameters by applying the CFD-based adjoint method [14]. During the further designing process, the air supply parameters of each inlet are controlled to be uniform for practical application.

2.3. Numerical method

The CFD-based adjoint method with area-constrained topology and cluster analysis was implemented in OpenFOAM [27]. This investigation adopted the finite volume method with staggered grids to discretize the Navier-Stokes equations and adjoint equations. The convection terms and diffusion terms of these two sets of equations were discretized by the first-order upwind scheme and the central difference scheme, respectively. This study then used the semi-implicit method for pressure-linked

equations (SIMPLE) algorithm [28] to couple the air/adjoint velocity and air/adjoint pressure in the discretized Navier-Stokes/adjoint equations.

3. Results

To verify the performance of the CFD-based adjoint method with area-constrained topology and cluster analysis for optimal design of an indoor environment, this study conducted the inverse design in a two-person office and a single-aisle, fully-occupied aircraft cabin.

3.1. Two-person office

Fig. 3 shows an office with displacement ventilation [29]. The original design [30] placed a single air supply inlet in the right wall near the floor as shown in Fig. 3. The air was exhausted through an outlet in the center of the ceiling. The heat sources in the office were the occupants, computers, and lamps. Because of the asymmetrical geometry and thermal conditions, one of the occupants might feel very comfortable while another might feel hot. Therefore, this study used the CFD-based adjoint method with area-constrained topology and cluster analysis to identify the optimal air supply inlet conditions that would improve the overall thermal comfort level in the occupant region. In the inverse design process, this study adopted Eq. (1) as the objective function and set the occupant region as the design domain Θ. The numerical simulation used a structured grid with 263,043 hexahedral cells, on the basis of our grid-independence test. The convergence criteria were that $J < 0.02$ or $|J_k - J_{k-1}| < \delta$ (where $k \geq 2$ and $\delta = 10^{-3}$), the average |PMV| in the design domain ($\overline{|PMV|}_\Theta$) should be less than 0.5, and the average PD in the design domain ($\overline{PD}_\Theta$) should be less than 15%.

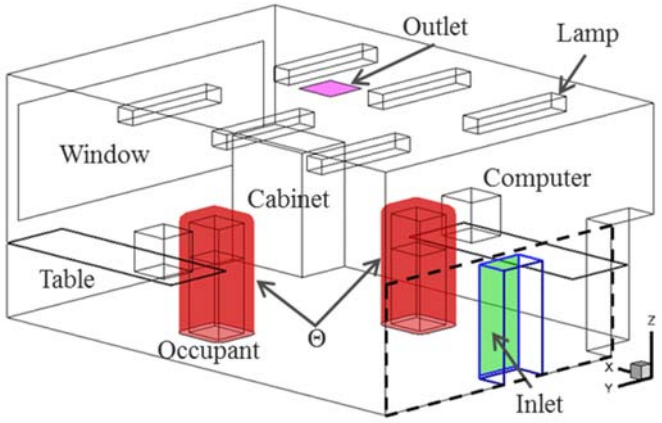

Fig. 3. Schematic of a two-person office

Using the above setup, this study first designed the air supply parameters (velocity and temperature) and assumed the initial air supply inlet to be the dashed area on the right wall as shown in Fig. 3 (enclosing potential locations for the optimal air supply inlets). Experimental data on thermo-fluid boundary conditions [30] were used for the other boundary conditions. As shown in Fig. 4, the objective function decreased gradually with successive design cycles. At design cycle 65, the convergence criteria were satisfied ($J = 0.0198$, $\overline{|PMV|}_\Theta = 0.12$, and $\overline{PD}_\Theta = 2.6\%$). As an example, Fig. 5 shows the variation of the PMV distribution around the occupants during the design process. With the initial design variables, the average |PMV| around the occupants

was 0.71 as shown in Fig. 5(a). After 65 design cycles, the average |PMV| around the occupants was 0.12 as shown in Fig. 5(b), which was lower than 0.5 [31].

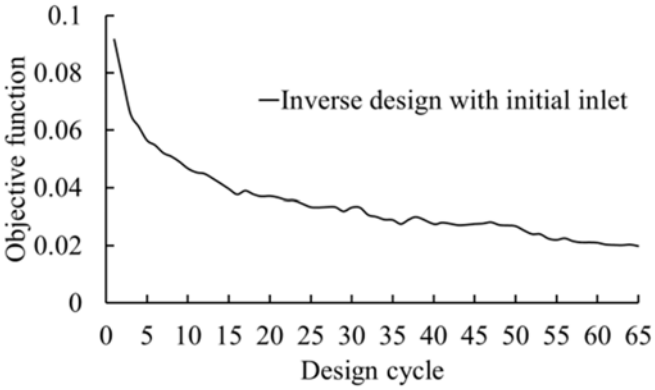

Fig. 4. Variation of the objective function with the design cycle during the inverse design process

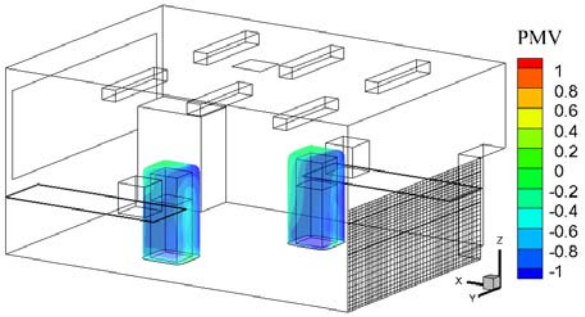

(a) PMV distribution at design cycle 1

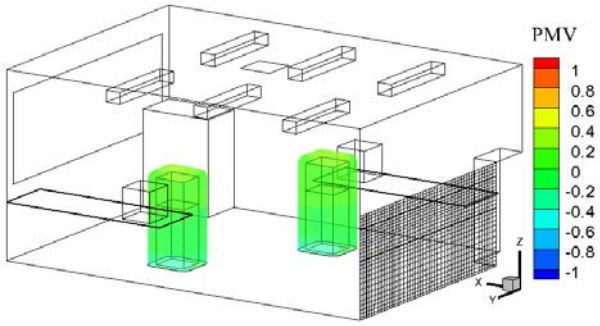

(b) PMV distribution at design cycle 65

Fig. 5. PMV distribution around the occupants at (a) design cycle 1 and (b) design cycle 65.

Meanwhile, Fig. 6(a) shows the distribution of air supply velocity at design cycle 65. This study then used the area-constrained topology optimization method to determine the number, size, and locations of the air supply inlets. To ensure reasonable air supply velocities, this investigation assumed the air supply flow rate to be in the range of 4 to 10 ACH and the air supply inlet size in the range of 0.145 to 0.51 m^2. The number, size, and locations of the resulting air supply inlets are depicted in Fig. 6(b).

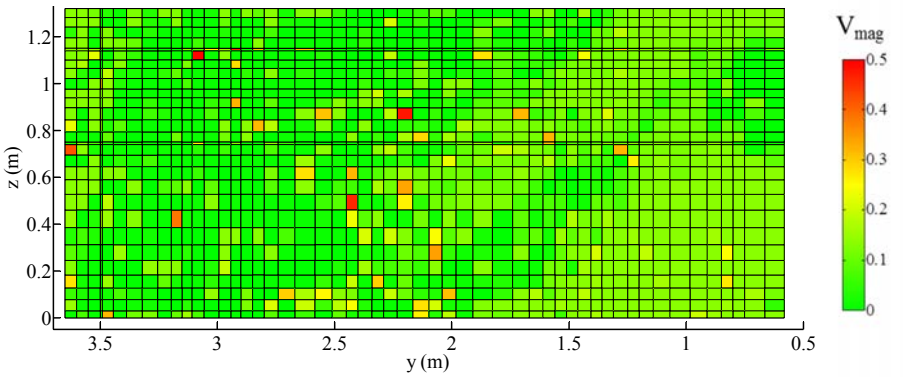

(a) Design cycle 65 by CFD-based adjoint method

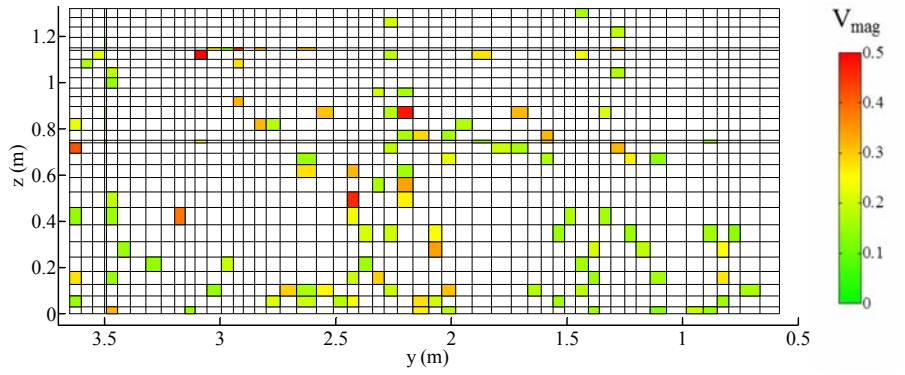

(b) Area-constrained topology applied

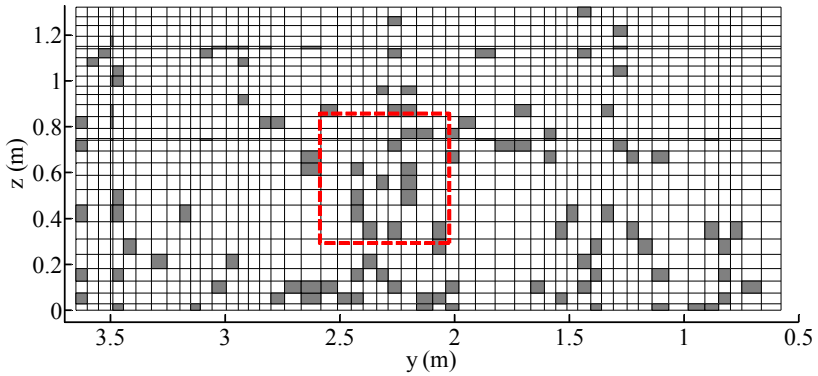

(c) Cluster analysis for one square air supply inlet

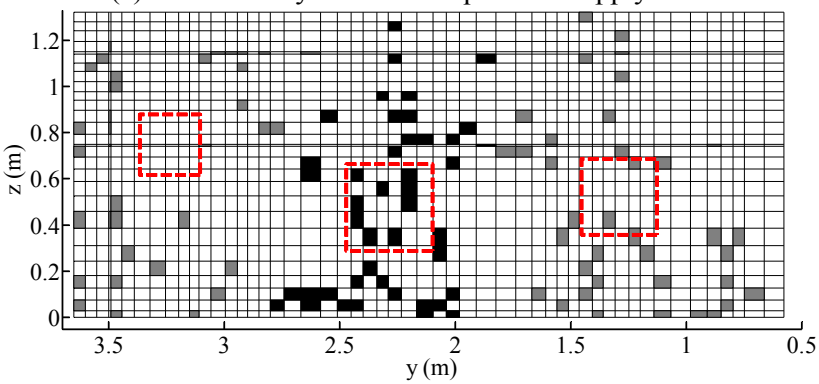

(d) Three square air supply inlets by cluster analysis

Fig. 6. Variation of air supply conditions by CFD-based adjoint method with

area-constrained topology and cluster analysis: (a) at design cycle 65 by CFD-based adjoint method, (b) with the application of area-constrained topology, (c) cluster analysis for one square air supply inlet, and (d) cluster analysis for three square air supply inlets

The number of air supply inlets was far too high for practical use. A lower number of inlets makes the engineering application easier. Therefore, centroid-based hierarchical cluster analysis was used to consolidate the inlets. The analysis first identified a single air supply inlet as shown in Fig. 6(c). With this inlet, we conducted forward CFD simulation and found that the corresponding objective function satisfied the convergence criteria (J = 0.020, $\overline{|PMV|}_{\Theta}$ = 0.16, and $\overline{PD}_{\Theta}$ = 2.2%). However, the use of a single air supply inlet may not always result in a sufficiently small corresponding objective function in other engineering applications. As an example, Fig. 6(d) shows how three air supply inlets were consolidated by cluster analysis. The grey air supply inlets on the left/right in Fig. 6(d) were consolidated into the inlets (red dashed lines) on the left/right. The black air supply inlets in the middle were consolidated into the inlet (red dashed lines) in the middle. The objective function of the case with three inlets also satisfied the convergence criteria (J = 0.019, $\overline{|PMV|}_{\Theta}$ = 0.16, and $\overline{PD}_{\Theta}$ = 2.0%).

On the basis of the single air supply inlet and the three inlets, the adjoint method was further used to optimize the air supply parameters (air temperature and velocity) and the shape of the inlets. This study set up the following cases:

- Case A: Inverse design of air supply parameters for the single air supply inlet
- Case B: Inverse design of air supply parameters for the three air supply inlets
- Case C: Inverse design of air supply parameters and shape for the single air supply inlet as shown in Fig. 8(c)
- Case D: Inverse design of air supply parameters and shape for the three air supply inlets as shown in Fig. 9(c)

Fig. 7 depicts the change in the objective functions of the four cases during the subsequent optimization process. By comparing Figs. 4 and 7, we find that the objective functions at design cycle 1 with the consolidated square air supply inlets was larger than that at design cycle 65 with the initial air supply inlet. This is because the cluster analysis significantly changed the location and shape of the inlets. After several design cycles, all the objective functions reached the convergence criteria ($|J|<0.02$, $\overline{|PMV|}_{\Theta} \leq 0.5$, and $\overline{PD}_{\Theta} \leq 15\%$). Note that the greater the number of air supply inlets, the better the thermal environment became in case B as compared with case A. However, case A can still produce a small objective function. In this particular case, a single air supply inlet was preferable because it was more practical than inlets.

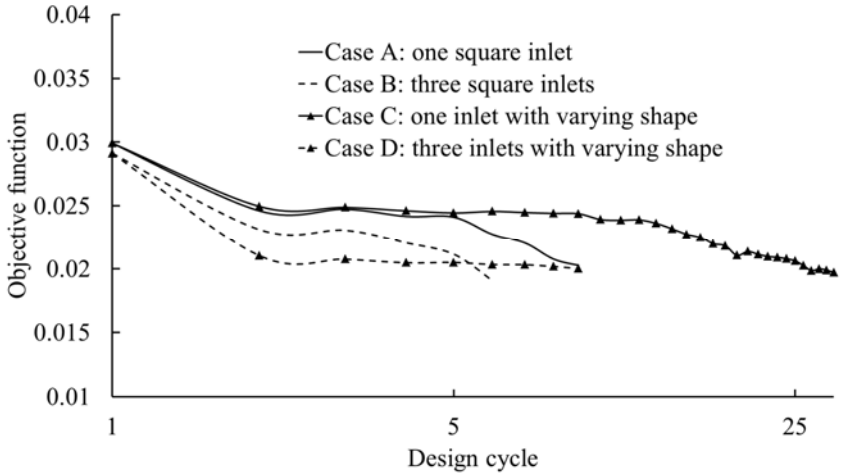

Fig. 7. Variation of objective function with design cycle during optimization of air supply parameters and inlet shape

Using PMV as an example, Figs. 8 and 9 show its distribution at the first and last design cycles for cases A, B, C, and D. The final designs of the four cases had very similar PMV distribution. The results for cases C and D were not better than the results for cases A and B, and the designed shapes for the air supply inlets were impractical.

The above results demonstrate that the proposed CFD-based adjoint method with area-constrained topology and cluster analysis can be used to identify the number, size, location, shape and air supply parameters of the inlets for the two-person office.

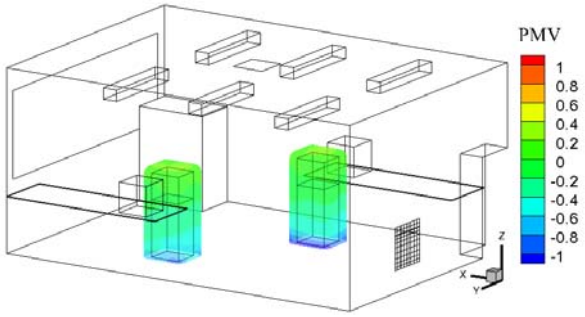

(a) Design cycle 1 of cases A and C

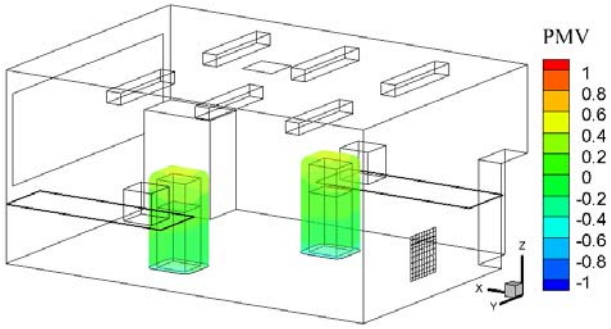

(b) Design cycle 9 of case A

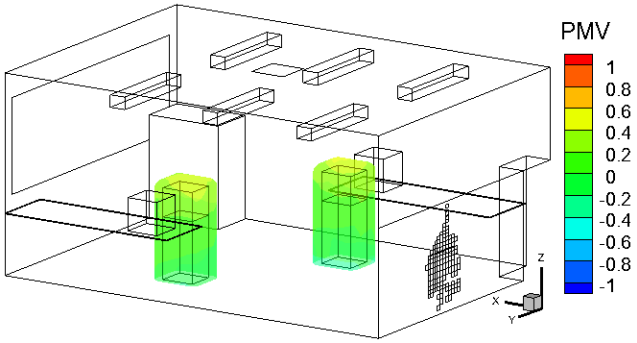

(c) Design cycle 30 of case C

Fig. 8. PMV distribution around the occupants at (a) design cycle 1 of cases A and C, (b) design cycle 9 of case A, and (c) design cycle 30 of case C.

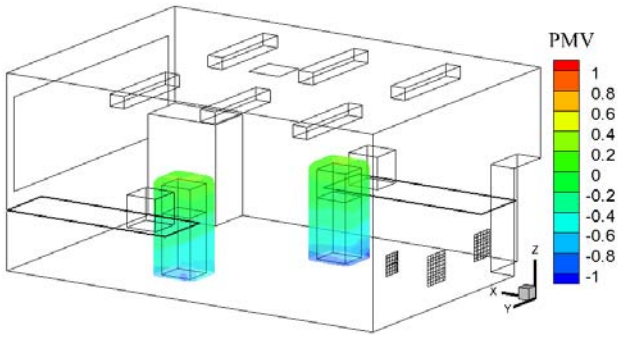

(a) Design cycle 1 of cases B and D

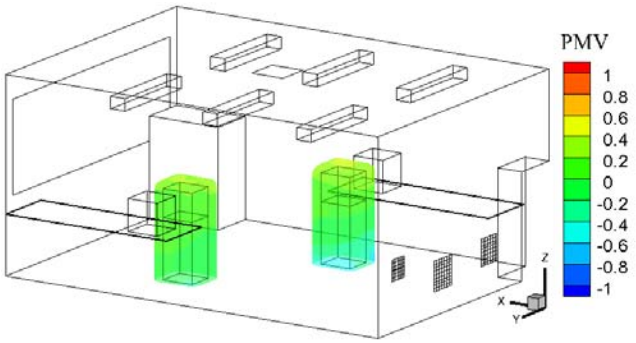

(b) Design cycle 6 of case B

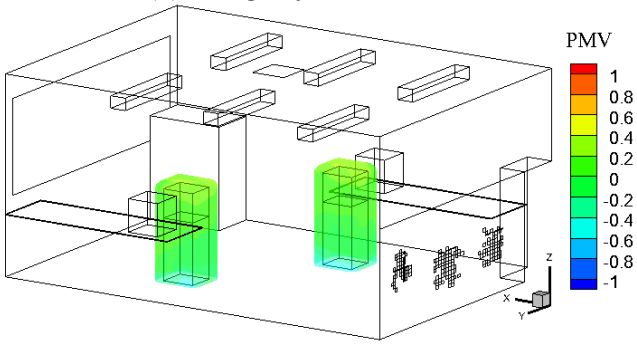

(c) Design cycle 9 of case D

Fig. 9. PMV distribution around the occupants at (a) design cycle 1 of cases B and D, (b) design cycle 6 of case B, and (c) design cycle 9 of case D.

3.2. Single-aisle, fully-occupied aircraft cabin

A single-aisle, fully-occupied aircraft cabin, as shown in Fig. 10 [32], was selected for further demonstration of the proposed method. The original air supply inlet was a slot placed in the sidewall near the ceiling. Fresh air was supplied through the air supply inlet and exhausted through an outlet at the bottom of the sidewall. For such a narrow aircraft cabin space and high-occupant-density environment, it was difficult for the original design to satisfy simultaneously three passengers' requirements for the thermal environment [15]. Therefore, this study used the CFD-based adjoint method with area-constrained topology and cluster analysis to design the number, size, and locations of the inlets and the air supply parameters. The objective function again employed Eq. (1), but PMV was replaced by PMV_c [15], which is an index for commercial airplanes. The design domain Θ was the surfaces around the three passengers at a distance of 0.1 m, as shown by the dark red color in Fig. 10.

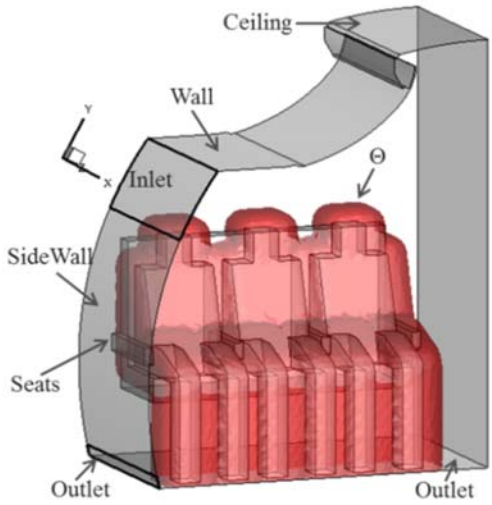

Fig. 10. Schematic of a single-aisle, fully-occupied aircraft cabin

The inverse design process first used the CFD-based adjoint method to identify the optimal air supply parameters when the area of the air supply inlet was that represented by the thick black line on the side wall in Fig. 10 (i.e., potential locations for air supply inlets). The initial inverse design set the air supply velocity as $V_{x,\,inlet}$ = 1.5 m/s, $V_{y,\,inlet}$ = 0, $V_{z,\,inlet}$ = 0, and air supply temperature as T_{inlet} = 17 ºC. All the other boundary conditions for the aircraft cabin used in this study came from Liu et al. [15]. The numerical simulation used a grid with three million unstructured cells according to our grid-independence test. The convergence criteria were set as $J < 0.02$ or $|J_k - J_{k-1}| < \delta$ (where $k \geq 2$ and $\delta = 10^{-3}$); the average $|PMV_c|$ in the design domain ($\overline{|PMV_c|}_{\Theta}$) should be less than 0.5; and the average PD in the design domain ($\overline{PD}_{\Theta}$) should be less than 15%. Fig. 11 shows the variation of the objective function with the number of design cycles. After 80 design cycles, convergence was achieved.

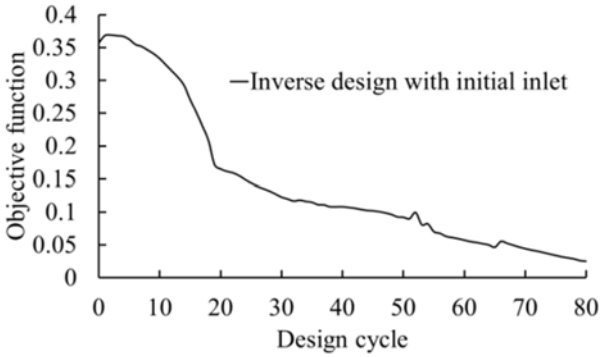

Fig. 11. Variation of the objective function with the number of design cycles in the inverse design process

Fig. 12 depicts the variation of the PMV_c distribution around the occupants when the air supply parameters were optimized. As shown in Fig. 12(a), the average $|PMV_c|$ around the occupants was 2.3 when the design process started. After 80 design cycles, the average $|PMV_c|$ around the occupants was only 0.14, as shown in Fig. 12(b).

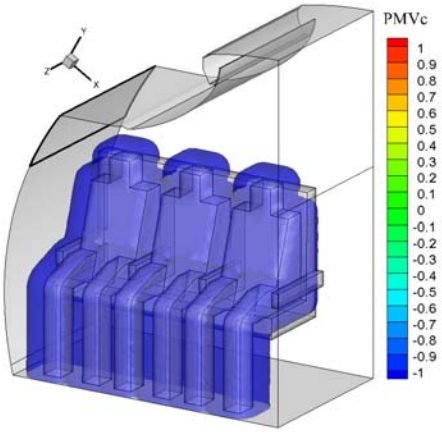

(a) PMV distribution at design cycle 1

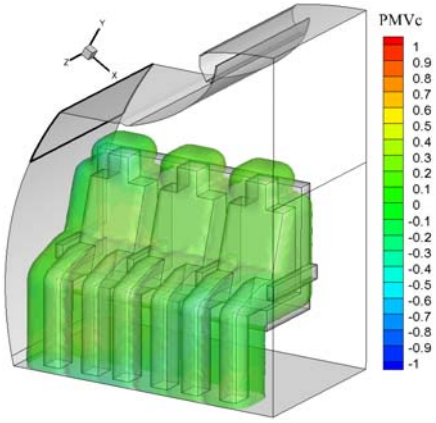

(b) PMV distribution at design cycle 80

Fig. 12. PMV distribution around the occupants at (a) design cycle 1 and (b) design cycle 80.

With the results at design cycle 80, this study used the area-constrained topology optimization method to determine the number, size, and location of the air supply inlets. The area constraint (0.009-0.43 m^2) for the inlets was determined by ANSI/ASHRAE Standard 161 [33] using Eqs. (10), (11), (12), and (13). We then clustered the air supply inlet number using the centroid-based hierarchical cluster analysis method. Figs. 13(a) and 13(b) show the size and location of a single square inlet and three rectangular inlets clustered, respectively. Note that we replaced the square with a rectangle, as shown in Fig. 13(b), because the centers of the consolidated air supply inlets were near the boundary of the initial area.

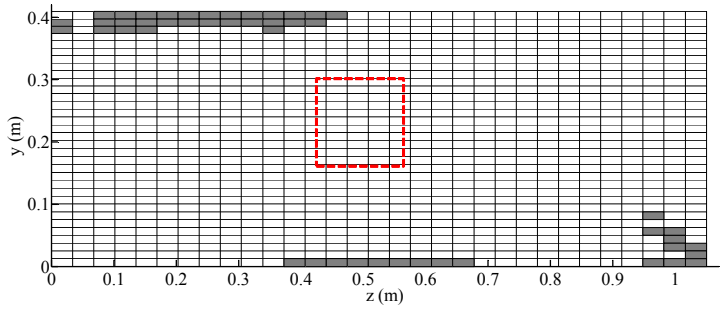

(a) One square air supply inlet

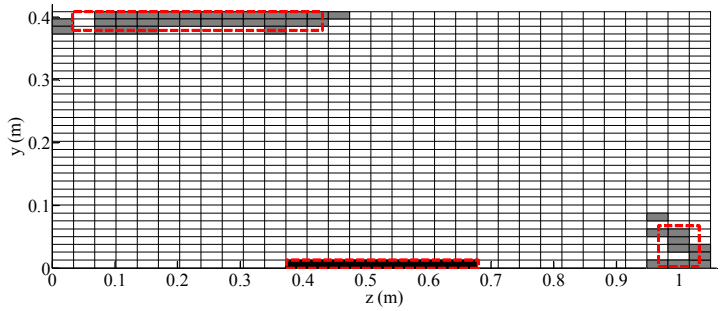

(b) Three air supply inlets

Fig. 13. The number, size, and location of the air supply inlets identified by area-constrained topology (grey region) and the consolidated air supply inlets determined by centroid-based hierarchical cluster analysis (enclosed by red dashed lines)

Next, with the consolidated air supply inlets, the adjoint method was used to optimize the air supply parameters:

- Case E: Inverse design of air supply parameters with one air supply inlet
- Case F: Inverse design of air supply parameters with three air supply inlets

Fig. 14 displays the change in the objective function during this optimization process. Each design cycle took about 12 hours to complete on a 12-core workstation with 32 GB memory. This investigation set a maximum of 30 design cycles and a design objective of $|J| < 0.02$, whichever was reached first. The results show that the greater the number of inlets, the smaller the objective function was. However, for such a narrow space in the single-aisle, fully-occupied aircraft cabin, installation of a large number of air supply inlets would be unrealistic. Hence, this investigation used a maximum of three inlets for the optimal design.

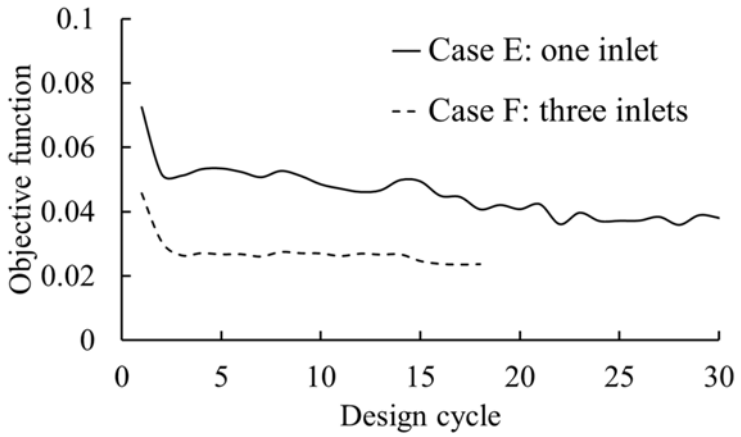

Fig. 14. Variation of the objective function with the design cycle during further optimization of the air supply parameters

Figs. 15 and 16 show the PMV_c distributions for cases E and F, respectively. We also found that the final designs of the two cases had very similar PMV_c distribution. Note that the greater the number of air supply inlets, the higher the thermal comfort level that could be achieved. Although the final design did not meet our requirements, the proposed CFD-based adjoint method with area-constrained topology and cluster analysis can be used to identify the number, size, and location of air supply inlets and the air supply parameters for optimizing the thermal environment in an aircraft cabin.

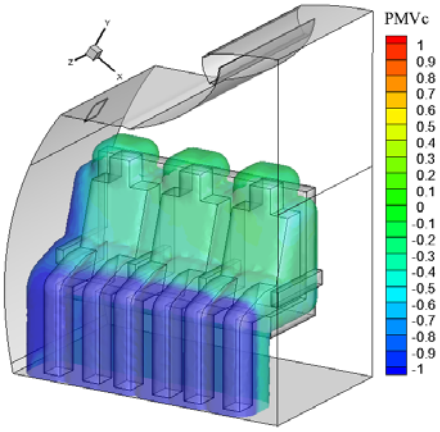

(a) Design cycle 1 of case E

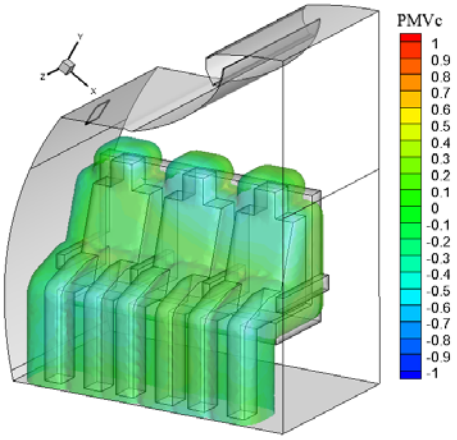

(b) Design cycle 30 of case E

Fig. 15. PMV distribution around the occupants at the initial (a) and final (b) design cycles when the air supply parameters were further optimized for case E

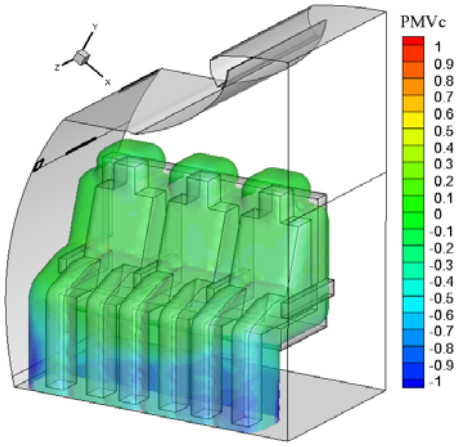

(a) Design cycle 1 of case F

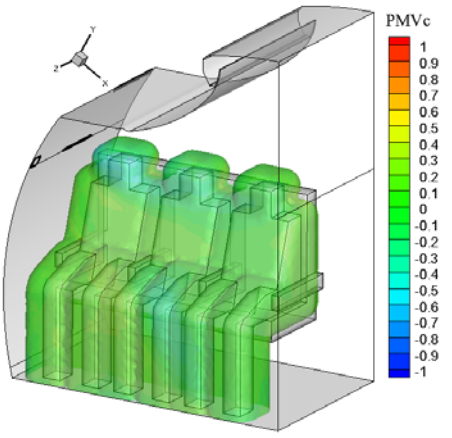

(b) Design cycle 18 of case F

Fig. 16. PMV distribution around the occupants at the initial (a) and final (b) design cycles when the air supply parameters were further optimized for case F

4. Discussion

This investigation constructed the objective function using PMV and PD, and

weighting factors from Ncube and Riffat [18]. If other design objectives, such as the age of air or contaminant concentration, were considered, the objective function could be constructed in the same way, and the principle of the design process would remain the same. More than two evaluation criteria could be used, but it would make identification of the optimal design more difficult.

Table 1 lists the area constraints and the areas of optimal air supply inlets for the two indoor spaces in this study. The area constraint that we introduced was a range rather than a single value. Any air supply area within this range is reasonable. This study determined the air supply area according to the distribution of air supply velocity indentified by the CFD-based adjoint method. The inlet cells with relatively small velocity value were closed and set as the wall boundary condition. Those inlet cells with relatively large air supply velocity remained unchanged.

Table 1. Area constraints and area of optimal air supply inlets for the two cases

	Area constraint (m^2)	Area of optimal air supply inlets (m^2)
Two-person office	0.145-0.51	0.31
Single-aisle, fully-occupied aircraft cabin	0.009-0.43	0.02

Cartesian coordinates were used as an example to verify the performance of the integrated CFD-based adjoint method and area-constrained topology and cluster analysis for inversely designing the indoor environment. Application of the method in other coordinate systems would be possible by taking a similar approach, although it could be more complicated.

This investigation conducted the inverse design on a 12-core workstation with 32 GB memory. Two days were required to finish the whole inverse design process for the two-person office case, and one month for the aircraft cabin case. The convergence speed of the design was slow because of the steepest descent method used in this study. To speed up the design procedure, one could try the exact Newton method or the quasi-Newton method.

5. Conclusions

This investigation combined the CFD-based adjoint method with an area-constrained topology and cluster analysis for the inverse design of an indoor environment. Use of the combined method to design the thermal environment in an office and an aircraft cabin led to the following conclusions:

- The method was able to identify the optimal number, location, and size of air supply inlets and the optimal air supply parameters under the given convergence criterion. The design produced a desirable thermal environment in the office and the aircraft cabin.
- The centroid-based hierarchical cluster analysis was able to consolidate the scattered air supply inlets determined by the area-constrained topology method into a limited number of inlets. A greater number of air supply inlets could produce a better thermal environment but might not be practical.

- The method was also able to determine the shape of the air supply inlets. However, for the applications discussed in this paper, the corresponding results were not better than the results without changing the shape of the air supply inlets. In addition, the shape might be too complicated for use in practice. Therefore, this investigation used a rectangular shape for the inlets.

Acknowledgement

This research was partially supported by the National Key Program of the Ministry of Science and Technology, China, on "Green Buildings and Building Industrialization" through Grant No. 2016YFC0700500 and by the National Natural Science Foundation of China through Grant No. 51478302.

References

[1] N.E. Klepeis, W.C. Nelson, W.R. Ott, J.P. Robinson, A.M. Tsang, P. Switzer, W.H. Engelmann, The National Human Activity Pattern Survey (NHAPS): A resource for assessing exposure to environmental pollutants [J], Journal of Exposure Science and Environmental Epidemiology. 11(3) (2001) 231.

[2] U.S. Department of Energy, Buildings Energy Data Book, Department of Energy, Washington DC, 2015.

[3] B. Guieysse, C. Hort, V. Platel, R. Munoz, M. Ondarts, S. Revah, Biological treatment of indoor air for VOC removal: Potential and challenges, Biotechnology Advances. 26(5) (2008) 398-410.

[4] W. Liu, T. Zhang, Y. Xue, Z. Zhai, J. Wang, Y. Wei, Q. Chen, State-of-the-art methods for inverse design of an enclosed environment, Building and Environment. 91 (2015) 91-100.

[5] J. Holland, Adaptation in natural and artificial systems: An introductory analysis with applications to biology, control and artificial intelligence, Quarterly Review of Biology. 6(2) (1975) 126-137.

[6] W.S. McCulloch, W. Pitts, A logical calculus of the ideas immanent in nervous activity, The Bulletin of Mathematical Biophysics. 5(4) (1943) 115-133.

[7] K. Li, H. Su, J. Chu, C. Xu, A fast-POD model for simulation and control of indoor thermal environment of buildings, Building and Environment. 60(60) (2013) 150-157.

[8] C. Othmer, A continuous adjoint formulation for the computation of topological and surface sensitivities of ducted flows, International Journal for Numerical Methods in Fluids. 58(8) (2008) 861-877.

[9] Q. Chen, Ventilation performance prediction for buildings: A method overview and recent applications, Building and Environment. 44 (2009) 848-858.

[10] Q. Chen, Z. Zhai, X. You, T. Zhang, Inverse Design Methods for Built Environment, Taylor & Francis Group, Oxford, England, 2017.

[11] Y. Xue, Z.J. Zhai, Q. Chen, Inverse prediction and optimization of flow control conditions for confined spaces using a CFD-based genetic algorithm, Building and Environment. 64 (2013) 77-84.

[12] T. Zhang, X. You, A simulation-based inverse design of preset aircraft cabin environment, Building and Environment. 82 (2014) 20-26.

[13] Y. Wei, T.T. Zhang, S. Wang, Prompt design of the air-supply opening size for a commercial airplane based on the proper orthogonal decomposition of flows, Building and Environment. 96 (2016) 131-141.

[14] W. Liu, M. Jin, C. Chen, Q. Chen, Optimization of air supply location, size, and parameters in enclosed environments using a computational fluid dynamics-based adjoint method, Journal of Building Performance Simulation. 9(2) (2016) 149-161.

[15] W. Liu, R. Duan, C. Chen, C.H. Lin, Q. Chen, Inverse design of the thermal environment in an airliner cabin by use of the CFD-based adjoint method, Energy and Buildings. 104(2) (2015) 147-155.

[16] P.O. Fanger, Thermal Comfort, Robert E. Kn'cger Publishing Company, Florida, 1982.

[17] P.O. Fanger, A.K. Melikov, H. Hanzawa, J. Ring, Air turbulence and sensation of draught, Energy and Buildings. 12(1) (1988) 21-39.

[18] M. Ncube, S. Riffat, Developing an indoor environment quality tool for assessment of mechanically ventilated office buildings in the UK - A preliminary study, Building and Environment. 53 (2012) 26-33.

[19] X. Zhao, W. Liu, S. Liu, Y. Zou, Q. Chen, Inverse design of an indoor environment using a CFD-based adjoint method with the adaptive step size for adjusting the design parameters, Numerical Heat Transfer, Part A: Applications. 71(7) (2017) 707-720.

[20] B.J.M. Ortega, W.C. Rheinboldt, Iterative Solution of Nonlinear Equations in Several Variables, Chap. 8, Academic Press, New York, 1970.

[21] S. Yamasaki, T. Nomura, A. Kawamoto, K. Sato, K. Izui, S. Nishiwaki, A level set based topology optimization method using the discretized signed distance function as the design variables, Structural and Multidisciplinary Optimization. 41(5) (2010) 685-698.

[22] M.Y. Wang, X. Wang, D. Guo, A level set method for structural topology optimization, Computer Methods in Applied Mechanics and Engineering. 192(1) (2003) 227-246.

[23] E.M. Papoutsis-Kiachagias, K.C. Giannakoglou, Continuous adjoint methods for turbulent flows, applied to shape and topology optimization: Industrial applications, Archives of Computational Methods in Engineering. 23(2) (2016) 255-299.

[24] C. Hinterberger, M. Olesen, Industrial application of continuous adjoint flow solvers for the optimization of automotive exhaust systems, An ECCOMAS Thematic Conference, Antalya, Turkey, 2011.

[25] ASHRAE. ASHRAE Handbook - HVAC Applications(SI). Atlanta: American Society of Heating, Refrigerating and Air Conditioning Engineers, 2011.

[26] S.K. Uppada, Centroid based clustering algorithms- A clarion study, International Journal of Computer Science and Information Technologies. 5 (6) (2014) 7309-7313.

[27] OpenFOAM. The Open Source CFD Toolbox, http://www.openfoam.com, 2012.

[28] S.V. Patankar, D.B. Spalding, A calculation procedure for heat, mass and

momentum transfer in three-dimensional parabolic flows, International Journal of Heat and Mass Transfer. 15 (10) (1972) 1787-1806.

[29] K. Lee, T. Zhang, Z. Zheng, Q. Chen, Comparison of airflow and contaminant distributions in rooms with traditional displacement ventilation and under-floor air distribution systems, ASHRAE Transactions. 115(2) (2009) 306-321.

[30] X. Yuan, Q. Chen, L. Glicksman, Y. Hu, X. Yang, Measurements and computations of room airflow with displacement ventilation, ASHRAE Transactions. (1999) 340-352.

[31] ISO 7730: 2005. Ergonomics of the Thermal Environment -- Analytical Determination and Interpretation of Thermal Comfort Using Calculation of the PMV and PPD Indices and Local Thermal Comfort Criteria, 2005.

[32] T. Zhang, P. Li, Y. Zhao, S. Wang, Various air distribution modes on commercial airplanes, part 2: CFD modeling and validation, HVAC&R Research. 19(5) (2013) 457-470.

[33] ASHRAE, Standard 161-2007. Air Quality Within Commercial Aircraft, ASHRAE, Inc, Atlanta, GA, 2007.